Power-Assist Control Switching from Adaptive Nonstationary Servo Control to Force Sensorless Nonstationary Impedance Control

Susumu Hara
Graduate School of Engineering,
Nagoya University
Furocho, Chikusa-ku,
Nagoya, Japan 464-8603
Email: haras@mech.nagoya-u.ac.jp

Yoji Yamada
Graduate School of Engineering,
Nagoya University
Furocho, Chikusa-ku,
Nagoya, Japan 464-8603
Email: yamada-yoji@mech.nagoya-u.ac.jp

Suwoong Lee
Intelligent Systems Research Institute,
National Institute of Advanced Industrial
Science and Technology
1-1-1 Umezono, Tsukuba, Ibaraki, Japan
305-8568
Email: lee-sirg@aist.go.jp

***Abstract* – Many power-assist systems for industrial uses possess simple power-assisting function only. The authors studied on the positioning method of a cart using a smooth switching from the servo access control for the conveyance function to the force sensorless impedance control (FSLIC) for the power-assisting function. The nonstationary optimal control method and the nonstationary impedance control law were applied. However, the optimal control method requires the offline calculations for generating time-varying feedback gains. For actual problems including parameter variations, this characteristic is inconvenient. From such a point of view, this study investigates the use of the adaptive nonstationary servo control (ANSSC) technique instead of the optimal control method. Therefore, this paper discusses the control method switching from ANSSC based access to FSLIC based power-assist. The effectiveness of this method is verified experimentally.**

I. Introduction

In spite of popularization of industrial robots, there are some processes which require operator's actions instead of the uses of autonomous robots. For example, many operators handle and position heavy objects in automotive assembly processes [1]. For that reason, various power-assist systems based on the impedance control have been developed [1]-[3].

If we consider many applications of power-assist systems, the positioning objects have been traveled to around the power-assist system by a conveyance system as shown in the operation type - I of Fig. 1. However, in order to improve the efficiency of operation and reduce the physical burden of operators, we should pay attention to the cooperation of both the conveyance and the power-assisting functions. It is ideal that both the automatic conveyance and the power-assist processes are realized by single actuator and the novel controller for the smooth switching of both the processes. It enables us to save control energy and improve operators' comfortable. The operation type - II of Fig. 1 shows its scheme. Hereafter, each process is called "mode" in this paper.

Taking that situation into account, the first author studied on the positioning of a cart by means of a smooth switching from the servo control mode (SCM) to the impedance control mode (ICM) in [4]. The smooth switching in this study means the continuous switching of the control inputs of plural control modes. For SCM design, Ref. [4] utilized LQI (Linear Quadratic Integral) control technique. For the purpose of the smooth switching, the braking mode (BM) was inserted between SCM and ICM. Both SCM and BM were designed simultaneously by means of the nonstationary optimal control method [5], [6]. A nonstationary impedance control technique was utilized for ICM. The smooth mode switchings as shown in Fig. 2 were realized by these techniques.

For the realization of the impedance control, Ref. [4] utilized a force sensor. This method assumes that the operator has to catch the specific part connected with the force sensor as shown in Fig. 2. If he/she misses to catch it, the cart continues to run for a while. Moreover, if the force sensor has some trouble at the moment that the operator catches the special part, the cart generates unpredictive motion. From such a problem, a force sensorless impedance control version for the previous method to improve the safety of operators was also proposed in [7]. The

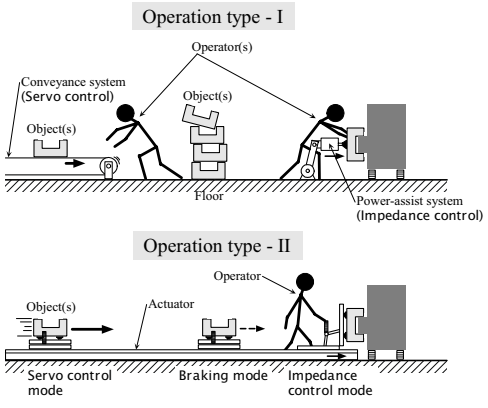

Fig. 1. Conveyance and power-assist processes.

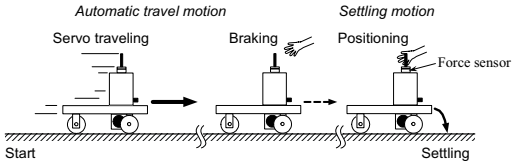

Fig. 2. Positioning operation.

use of the dual control system based on the methods in [4] and [7] can improve the functional safety of the system.

However, the nonstationary optimal control method for SCM/BM design requires the offline computations of a time-varying Riccati equation to obtain time-varying feedback gains. Hence, if a controlled object parameter such as mass often varies in a wide range, considerable kinds of time-varying Riccati equations have to be solved offline and the feedback gains have to be saved in computer memories a priori. This case increases the load of implementation seriously. Most power-assist systems are used for transferring many kinds of heavy objects. Then, the object mass often varies in the wide range between empty and maximum heavy value.

As a method similar to the nonstationary optimal control method, the first author proposed the Adaptive Nonstationary Control (ANSC) method and its application to positioning of vibration systems [8], [9]. The ANSC method is not the optimal control based on criterion functions. However, it generates responses similar to the optimal control results. Moreover, it enables us to solve the time-varying Riccati equation online/real-time and adapt varying parameters. Then, this paper discusses the positioning control switching from the Adaptive Nonstationary Servo Control (ANSSC) to the Force Sensorless Impedance Control (FSLIC) on the basis of [7] and [8], [9]. In order to establish truly useful and safety mode switching type control method and improve the efficiency of novel type power-assist systems, we should verify the validity of this switching control method. The effectiveness of this switching method is verified experimentally.

II. The Cart in This Study

This study utilizes the cart in Fig. 3. It was adopted as a controlled object example in [4]. For further details of the cart and its modeling, the reader should refer to [4]. The photo of the cart is shown in Fig. 4. This cart possesses three wheels, a DC servomotor with encoder, and gears. The two front wheels are driving wheels. The other one is an auxiliary wheel. A handle with a force sensor is installed on the top of the cart. The operator positions the cart by catching the handle. Simultaneously, the operator's force is detected by the force sensor. An acceleration pickup is installed on the cart. The parameters of the cart are summarized in Table I. In experiments, the angular displacement and the angular velocity of the motor, the acceleration of the cart, and the force of the operator are detected. The acceleration signal is passed through a low-pass filter (three poles Bessel type, the cut of frequency: 3.0 Hz) in order to reduce the influence of noises. A DSP (TMS320C31) processes the control algorithm. Its sampling period is 1.0 ms. Real control input is given as the voltage of the motor.

If we neglect the Coulomb friction of the driving system, we can describe the model of the cart by Fig. 5. We define $x(t)$, $F(t)$, and $i(t)$ in Fig. 5 as the displacement of the cart [m], the horizontal force of the cart [N], and the current of the motor [A], respectively. Here, we obtain the following model [4]:

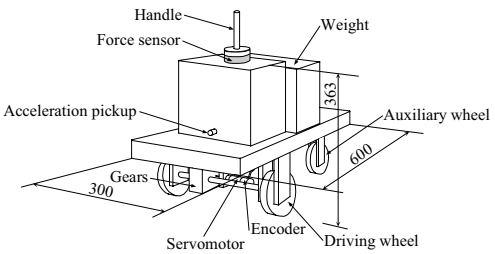

Fig. 3. Cart - a controlled object example.

Fig. 4. Photo of the cart.

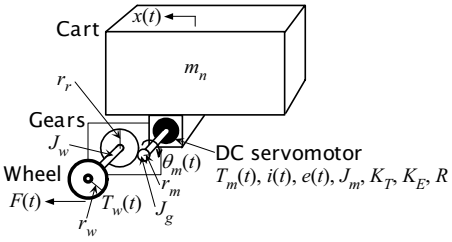

Fig. 5. Controlled object model.

TABLE I
Parameters of the Controlled Object

m_n	Mass of the model	20.0 kg (Nominal) - 50.0 kg (Max)
J_m	Moment of inertia of the motor	2.13 x 10^{-5} kg · m^2
J_g	Moment of inertia of the motor side gear	8.47 x 10^{-5} kg · m^2
J_w	Moment of inertia of the wheels	4.56 x 10^{-4} kg · m^2
$\alpha = r_r/r_m$	Gear ratio	15.0
r_w	Radius of the wheel	0.045 m
K_T	Torque constant of the motor	0.18 N · m/A
K_E	Back electromotive force constant of the motor	0.18 V · s/rad
R	Resistance of the motor	12.1 Ω

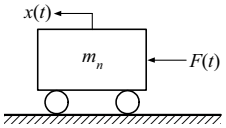

Fig. 6. Simple model.

$$\ddot{\theta}_m(t) = -\frac{\alpha K_T K_E}{r_w I_l R}\dot{\theta}_m(t) + \frac{\alpha K_T}{r_w I_l R} e(t) \quad (1)$$

$$I_l = \frac{r_w}{\alpha} m_n + \frac{\alpha}{r_w}\left(J_m + J_g + \frac{J_w}{\alpha^2} \right). \quad (2)$$

$\theta_m(t)$ and $e(t)$ mean the angular displacement [rad] and the input voltage [V] of the motor, respectively.

Moreover, let us get more simple model as shown in Fig. 6 to design the controller easily. This model corresponds to the double-integrator system. In order to obtain this simple version, the voltage $e(t)$ has to be given by

$$e(t)=\frac{R}{K_T}\left(J_m+J_g+\frac{J_w}{\alpha^2}\right)\ddot{\theta}_m(t)+K_E\dot{\theta}_m(t)+\frac{r_wR}{\alpha K_T}F(t). \quad (3)$$

In this study, we assume that each parameter can be identified accurately and the feedback loops in (3) can be realized. Then, this simple version is adopted as the controlled object model. The angular acceleration of the motor is obtained by cart acceleration measurement in experiments. The state equation of the model becomes as follows:

$$\dot{\boldsymbol{x}}(t)=\boldsymbol{A}\boldsymbol{x}(t)+\boldsymbol{b}F(t) \quad (4)$$
$$\boldsymbol{x}(t)=\begin{bmatrix}x(t)\\ \dot{x}(t)\end{bmatrix},\ \boldsymbol{A}=\begin{bmatrix}0 & 1\\ 0 & 0\end{bmatrix},\ \boldsymbol{b}=\begin{bmatrix}0\\ 1/m_n\end{bmatrix}.$$

III. The Control Method

This study assumes that the cart moves about 1.8 m distance. We switch the control mode from SCM to ICM via BM as shown in Fig. 2.

A. SCM

LQI control is applied to SCM. The velocity reference $r(t)$ is given. We define new variable $x_{sv}(t)$ as $\int\left[r(t)-\dot{x}(t)\right]dt$ and make the augmented system of (4) and $x_{sv}(t)$ as follows:

$$\dot{\boldsymbol{x}}_a(t)=\boldsymbol{A}_a\boldsymbol{x}_a(t)+\boldsymbol{b}_aF(t)+\boldsymbol{b}_rr(t) \quad (5)$$
$$\boldsymbol{x}_a(t)=\begin{bmatrix}\boldsymbol{x}(t)\\ x_{sv}(t)\end{bmatrix},\ \boldsymbol{A}_a=\begin{bmatrix}\boldsymbol{A} & \boldsymbol{0}\\ -\boldsymbol{c} & 0\end{bmatrix},\ \boldsymbol{b}_a=\begin{bmatrix}\boldsymbol{b}\\ 0\end{bmatrix},\ \boldsymbol{b}_r=\begin{bmatrix}\boldsymbol{0}\\ 1\end{bmatrix},\ \boldsymbol{c}=\begin{bmatrix}0 & 1\end{bmatrix}.$$

LQI control means the LQ optimal control problem for (5) under the following criterion function:

$$J_{LQI}=\int_0^\infty\left[\boldsymbol{x}_a^{\mathrm{T}}(t)\boldsymbol{Q}_{LQI}\boldsymbol{x}_a(t)+r_{LQI}F^2(t)\right]dt \quad (6)$$

where $\boldsymbol{Q}_{LQI}$ and r_{LQI} are time-invariant weights. For further details of this subsection, the reader should refer to [4].

B. Unified Design of SCM and BM

Taking the switching from SCM to ICM into account, we should extinguish the feedback loop on the servo variable $x_{sv}(t)$ at some time before ICM. However, abrupt switching may bring serious danger to the operator. Reference [4] introduces BM in order to avoid the abrupt switching. BM possesses the velocity feedback only and is obtained by the weight on the velocity only. To realize the smooth transition from SCM to BM, the following time-varying Riccati equation using time-varying weights $\boldsymbol{Q}(t)$ was introduced in [4].

$$-\dot{\boldsymbol{P}}(t)=\boldsymbol{P}(t)\boldsymbol{A}_a+\boldsymbol{A}_a^{\mathrm{T}}\boldsymbol{P}(t)-\boldsymbol{P}(t)\boldsymbol{b}_a\boldsymbol{b}_a^{\mathrm{T}}\boldsymbol{P}(t)+\boldsymbol{Q}(t)$$
$$\boldsymbol{P}(t_f)=\boldsymbol{0},\ \left(t\in\left[0,t_f\right]\right) \quad (7)$$

As the elements of $\boldsymbol{Q}(t)$, we consider two time-varying variables $q_b(t)$ and $q_s(t)$ for the velocity and the servo variable, respectively. $\boldsymbol{Q}(t)$ is given by

$$\boldsymbol{Q}(t)=\mathrm{diag}\begin{bmatrix}0 & q_b(t) & q_s(t)\end{bmatrix}. \quad (8)$$

The control input is obtained by the following feedback control law using time-varying feedback gains $\boldsymbol{f}_b(t)$:

$$F(t)=-\boldsymbol{f}_b(t)\boldsymbol{x}_a(t),\ \boldsymbol{f}_b(t)=\boldsymbol{b}_a^{\mathrm{T}}\boldsymbol{P}(t). \quad (9)$$

This algorithm corresponds to the nonstationary optimal control problem for the following time-varying criterion function [6]:

$$J=\int_0^{t_f}\left[\boldsymbol{x}_a^{\mathrm{T}}(t)\boldsymbol{Q}(t)\boldsymbol{x}_a(t)+F^2(t)\right]dt. \quad (10)$$

$q_s(t)$ is set to a large value during SCM and $q_b(t)$ enlarges in the vicinity of BM. For the smooth switching, $q_s(t)$ becomes very small at the end of SCM. Simultaneously, the feedback gain on the variable $x_{sv}(t)$ approaches 0.

However, time-varying Riccati equation (7) has to be solved by reversed time $\left(t:t_f\to 0\right)$ calculations under appropriate time-varying weights $\boldsymbol{Q}(t)$ and the boundary condition. And we have to save the time-varying feedback gains into the computer memories a priori in the previous method. Therefore, if a controlled object parameter such as mass often varies in wide range, the load of implementation is extremely increased. For such a problem, the Adaptive Nonstationary Servo Control (ANSSC) method proposed by the first author [8], [9] is applied to SCM/BM in this paper. Generally, the mass of the controlled object can be measured by using a loadcell. Then, we assume that all the parameters of the controlled object are time-invariant and can be determined at the starting time of control. Here, the following Riccati equation instead of (7) is solved by progressive time $\left(t:0\to t_f\right)$ calculations:

$$\frac{d\boldsymbol{P}'(\tau)}{d\tau}=\boldsymbol{P}'(\tau)\boldsymbol{A}_a+\boldsymbol{A}_a^{\mathrm{T}}\boldsymbol{P}'(\tau)-\boldsymbol{P}'(\tau)\boldsymbol{b}_a\boldsymbol{b}_a^{\mathrm{T}}\boldsymbol{P}'(\tau)+\boldsymbol{Q}'(\tau) \quad (11)$$

where $\boldsymbol{Q}'(\tau)=\boldsymbol{Q}(t=\tau)$. The control input is

$$F(t)=-\boldsymbol{f}_b'(t)\boldsymbol{x}_a(t),\ \boldsymbol{f}_b'(t)=\boldsymbol{b}_a^{\mathrm{T}}\boldsymbol{P}'(\tau=t). \quad (12)$$

The initial condition $\boldsymbol{P}'(0)$ is given by $\boldsymbol{P}'(0)=\boldsymbol{0}$ or time-invariant solution matrix of general LQ control problem based on $\boldsymbol{Q}'(0)$ [10]. The control using (11) is not optimal control based on (10). However, this control generates responses similar to the optimal control results. Moreover, it enables us to solve

the time-varying Riccati equation online/real-time and adapt varying parameters easily.

C. Force Sensorless Control Based ICM

In ICM of [4], a simple impedance control method similar to that of [1] was utilized. This subsection also discusses the ICM design. Let us set the impedance characteristic for the operator in ICM as follows:

$$m_d \ddot{x}(t) + c_d \dot{x}(t) = F_h(t) \tag{13}$$

where m_d and c_d are the impedance parameters as mass and damping, respectively. $F_h(t)$ means the operator's force to the cart. The operator feels that the system seems to indicate the dynamics (13) by applying proper impedance control. To obtain this characteristic, the control input can be selected as follows:

$$F(t) = -\frac{m_n}{m_d} c_d \dot{x}(t) + \left(\frac{m_n}{m_d} - 1 \right) F_h(t). \tag{14}$$

However, when we calculate the control input by (14), we have to use a force sensor to detect the operator's force. It remains some safety problems as mentioned in Section 1. Reference [7] proposed another impedance control method by referring to [11]. The following impedance control law based on acceleration measurement was applied in [7]:

$$F(t) = (m_n - m_d)\ddot{x}(t) - c_d \dot{x}(t). \tag{15}$$

Equation (15) generates the same impedance control input as (14). However, if the driving system possesses Coulomb friction, the performance of impedance control using (15) worsens in comparison with the case using (14). Then, Ref. [7] assumed that the controlled object possesses some estimation mechanism of operation direction. An example of this mechanism is indicated in Fig. 7. This mechanism can detect the direction for which the operator pushes or pulls. Most power-assist systems require "enable switches (Hold-to-Run switches)" to input operator's intention to use. The estimation mechanism can be also adopted as the enable switch. Additional friction compensation force F_f according to the estimated operation direction is applied to the system. F_f is feedforward control input force. Its value is determined by some friction identification test a priori. When any directions are not estimated, F_f is set to 0.

D. Smooth Switching from BM to ICM

This subsection discusses a smooth switching method from BM to ICM in this paper. In [7], at some time during BM, the feedback gains can be described as:

$$\boldsymbol{f}_b(t_{sw}) \approx \begin{bmatrix} 0 & f_{bv}(t_{sw}) & 0 \end{bmatrix} \tag{16}$$

where $t = t_{sw}$ means the switching time of both the modes. ICM requires two kinds of feedback loops, on the acceleration and the velocity. Then, the following nonstationary impedance control method is utilized:

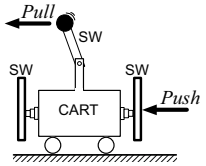

Fig. 7. Scheme of the estimation mechanism of operation direction.

$$F(t) = \left[m_n - m_d(t) \right] \ddot{x}(t) - c_d(t) \dot{x}(t). \tag{17}$$

If we choose $m_d(t_{sw}) = m_n$ and $c_d(t_{sw}) = f_{bv}(t_{sw})$, the control inputs of both the modes are equivalent at $t = t_{sw}$. We change these variables into their ideal values m_{dsett} and c_{dsett} smoothly by using sigmoid functions after $t = t_{sw}$.

However, different from the previous case, when $q_s(t)$ becomes zero, the feedback gain on the servo variable $f'_{bs}(t)$ is still not zero in the ANSSC method based on (11). Hence, we can not describe $\boldsymbol{f}_b(t_{sw})$ as (16). Here, let us take the control input generated by remaining $f'_{bs}(t)$ at $t = t_{sw}$ into account as follows:

$$F_{sv}(t_{sw}) = -f'_{bs}(t_{sw}) x_{sv}(t_{sw}). \tag{18}$$

Equation (19) is utilized for $c_d(t)$.

$$\begin{aligned} c_d(t) &= f'_{bv}(t_{sw}) - F_{sv}(t_{sw}) / \dot{x}(t_{sw}) \\ &+ \left[c_{dsett} - f'_{bv}(t_{sw}) + F_{sv}(t_{sw}) / \dot{x}(t_{sw}) \right] / \left\{ 1.0 + \exp\left[-\alpha \left(t_{sig} - \beta \right) \right] \right\} \end{aligned} \tag{19}$$

α and β are constants which determine the shape of $c_d(t)$. t_{sig} is $t - t_{sw}$. The value of (19) becomes $c_d(t_{sw}) = f'_{bv}(t_{sw}) - F_{sv}(t_{sw}) / \dot{x}(t_{sw})$ at $t = t_{sw}$. This means that (19) consists of the original elements in [7] and the adjusting elements for $F_{sv}(t_{sw})$. $F_{sv}(t_{sw})$ is not large input in comparison with the real control input in most cases because $f'_{bs}(t)$ is reduced during BM. Therefore, the responses after the mode switching are similar to those of the previous method case.

IV. Experiments

In order to verify the effectiveness of the proposing mode switching method, this section discusses experiments using the cart in Fig. 3. m_n is 20.0 kg in these experiments. Time-varying weights $q_s(t)$ (on the servo variable) and $q_b(t)$ (on the velocity) are determined by using sigmoid functions as follows (Fig. 8 (a) and (b)):

$$\begin{aligned} q_s(t) &= 1.0 \times 10^6 / \left\{ 1.0 + \exp\left[-280.0 (4.8 - t) \right] \right\} \\ q_b(t) &= \begin{cases} 5.0 \times 10^3 / \left\{ 1.0 + \exp\left[-2.0 (t - 6.8) \right] \right\} & (t < 6.2) \\ \gamma(t) / \left\{ 1.0 + \exp\left[-2.0 (t - 6.8) \right] \right\} & (6.2 \le t < 6.7) \\ 0.25 \quad (t \ge 6.7) \end{cases} \end{aligned} \tag{20}$$

$$\gamma(t) = 0.5 + \left(5.0\times10^{3} - 0.5\right)\frac{6.7 - t}{0.5}.$$

These weights are tuned by referring to the first author's previous study [4]. The time-varying feedback gains obtained by (11) with these weights are shown in Fig. 8 (c) and (d). Here, we set $\boldsymbol{P}'(0) = \boldsymbol{0}$. Different from [4] and [7], the feedback gain on $x_{sv}(t)$ [Fig. 8(c)] is not zero for a while after $q_s(t)$ becomes zero. These feedback gains are obtained real-time/online in actual experiments. According to [4], m_{dsett} and c_{dsett} are set to 2.0 kg and 5.0 N•s/m, respectively. α and β in (19) are set to 80.0 and 0.0875 respectively. $m_d(t)$ is tuned as follows:

$$m_d(t) = m_n + \left(m_{dsett} - m_n\right) / \left\{1.0 + \exp\left[-80.0\left(t_{sig} - 0.0875\right)\right]\right\}. \tag{21}$$

The shapes of $m_d(t)$ and $c_d(t)$ are similar to those of [4]. During BM, once the operator's force becomes larger than ± 1.5 N, the control mode is switched to ICM. In the experiments, the force sensor corresponds to the estimation mechanism. When $|F_h(t)| > 1.0$ N, the friction compensation force $F_f = 14.7$ N (constant) is added according to the estimated operation direction. For SCM, we use the velocity reference whose acceleration and constant speed are 0.2 m/s^2 and 0.4 m/s, respectively.

An experimental result is shown in Fig. 9. Figure 9 indicates (a): the displacement of the cart $x(t)$; (b): the velocity of the cart $\dot{x}(t)$; (c): the current of the motor $i(t)$; (d): the control input voltage $e(t)$; (e): the acceleration signal of the cart; and (f): the force of the operator $F_h(t)$, respectively. The displacement of the cart at $t = 10.0$ s is defined as $x = 0.0$ m. We can see the vibration phenomena during SCM in the cart velocity, the control input voltage, and the cart acceleration. However, another previous study [12] confirmed that these vibrations are caused by the mechanical imperfection of the cart.

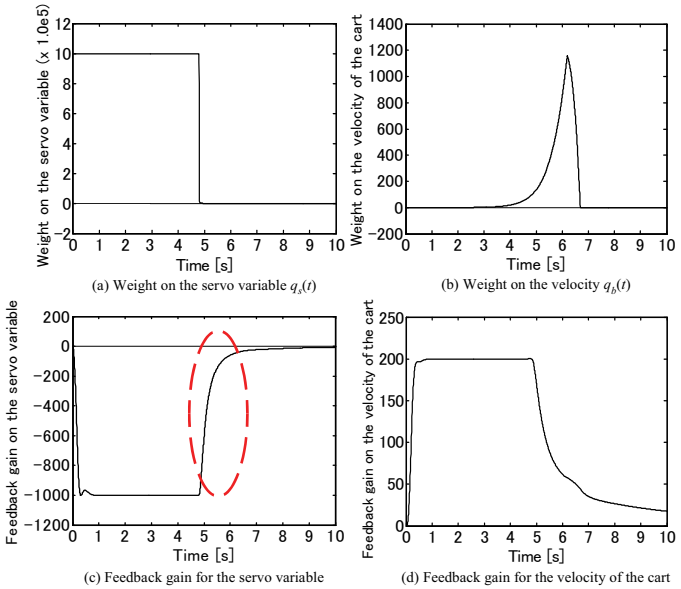

Fig. 8. Time-varying weights and feedback gains for SCM and BM.

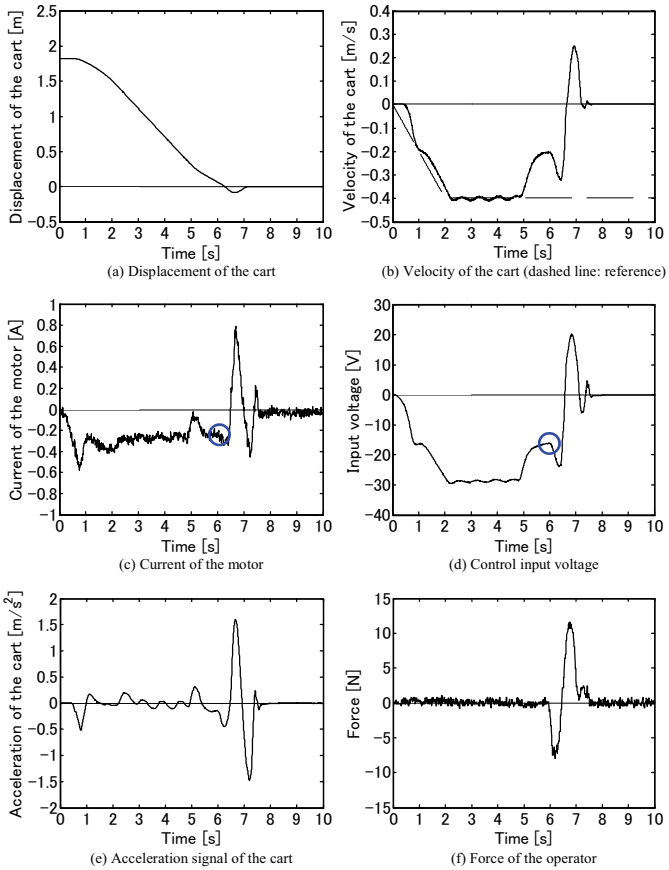

Fig. 9. Experimental result.

This result indicates that BM is smoothly switched to ICM when the operator holds the handle at about 6 seconds. No current and voltage saturations appear in Fig. 9. These responses are continuous at that time. Figure 10 shows the real feedback gain on the cart velocity. This gain corresponds to the feedback gain of ANSSC $f'_{bv}(t)$ between $t = 0$ and $t = t_{sw}$, the interpolation gain $\left[m_n / m_d(t)\right]c_d(t)$ between the braking control and the impedance control, and the impedance control gain $\left(m_n / m_{dsett}\right)c_{dsett}$ after the interpolation. It is remarkable point that the responses are continuous although the real velocity feedback gain varies abruptly at $t = t_{sw}$.

For your reference, a manual motion result without control is shown in Fig. 11. This figure indicates the trajectories when an operator pushes the cart for one direction about 5 cm and pulls back about 1 cm. Instead of the short distance movement, the operator requires about 20-30 N in Fig. 11(d). Moreover, the control result using the force sensor instead of the acceleration measurement is shown in Fig. 12. The operator's force can be reduced by using the force sensor in comparison with the case in Fig. 9. However, if we compare the operator's forces between the cases of Fig. 9 and Fig. 11, it is obvious that the proposing switching method realizes power-assisting. Therefore, the meaningfulness of the mode switching method from ANSSC to FSLIC is verified.

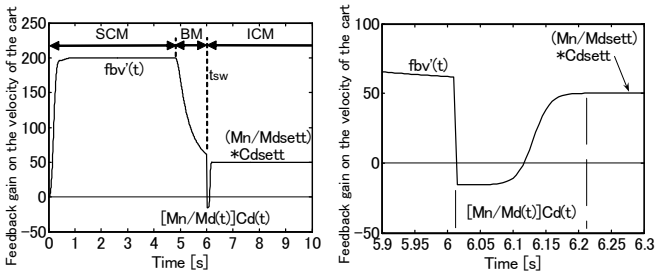

(a) Real feedback gain on the velocity of the cart (b) Enlargement of Fig. (a)

Fig. 10. Real feedback gain on the velocity of the cart in the case of Fig. 9.

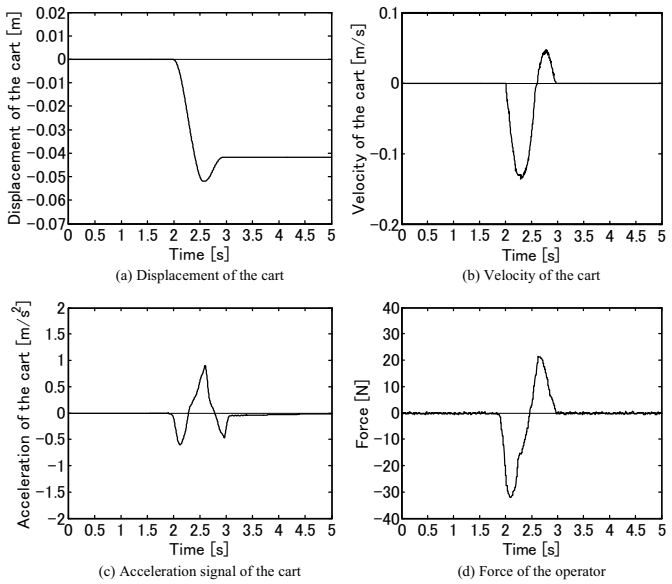

(a) Displacement of the cart (b) Velocity of the cart

(c) Acceleration signal of the cart (d) Force of the operator

Fig. 11. Manual motion of the cart.

V. Conclusion

Taking recent applications of power-assist systems to manufacturings into account, this study discussed the positioning method based on a smooth switching from the servo control mode to the impedance control mode. This study introduces the mode switching from the adaptive nonstationary servo control (ANSSC) to the force sensorless impedance control (FSLIC). The load of implementation can be reduced by using ANSSC in comparison with the conventional optimal control based method. The effectiveness of the method was verified experimentally.

Acknowledgment

This work was supported in part by Toyota Auto Body Co., Ltd.

References

[1] Y. Yamada, H. Konosu, T. Morizono, and Y. Umetani, "Proposal of skill-assist : a system of assisting human workers by reflecting their skills in positioning tasks," in *Proc. 1999 IEEE Int. Conf. Systems, Man, Cybernetics*, Tokyo, Japan, 1999, vol. IV, pp. 11-16.

[2] H. Nakamura and T. Honda, "Power assist system for a industrial use," *J. Soc. Inst. Contr. Eng.*, vol. 45, no. 5, pp. 445-448, 2006.

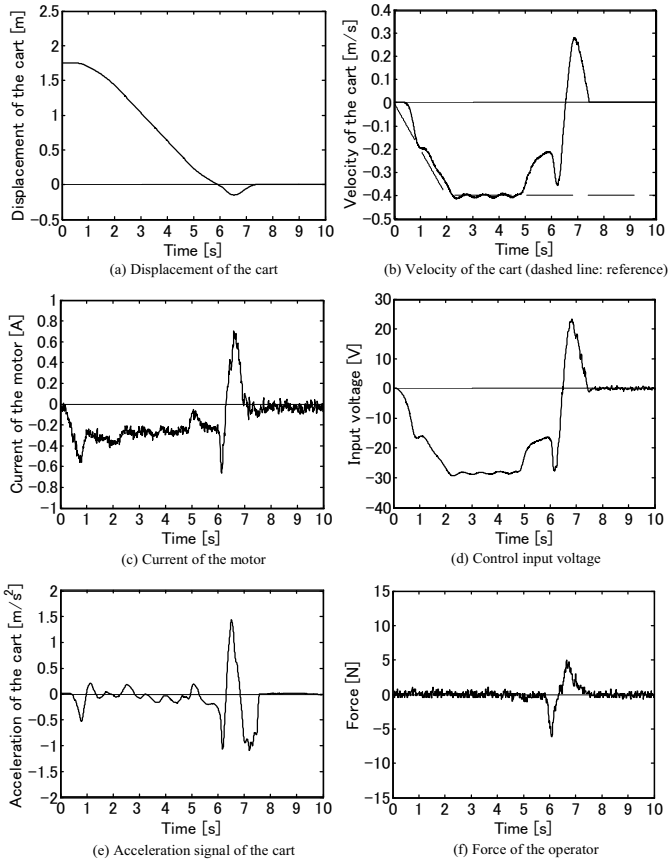

(a) Displacement of the cart (b) Velocity of the cart (dashed line: reference)

(c) Current of the motor (d) Control input voltage

(e) Acceleration signal of the cart (f) Force of the operator

Fig. 12. Experimental result (Force sensor is used.).

[3] H. Okuda, S. Hayakawa, T. Suzuki, and N. Tsuchida, "Modeling of human behavior in man-machine cooperative system based on hybrid system framework," in *Proc. 2007 IEEE Int. Conf. Robotics Automation*, Roma, Italy, 2007, pp. 2534-2539.

[4] S. Hara, "Positioning of a cart by means of a smooth switching from servo access control to impedance control," in *Proc. 2004 IEEE Conf. Robotics, Automation Mechatronics*, Singapore, 2004, pp. 588-594.

[5] S. Hara, "Unified design of time-varying gain type access control and integral type servo control by means of nonstationary optimal control method," *Microsyst. Technol.*, vol. 11, no. 8-10, pp. 676-687, 2005.

[6] S. Hara, "Nonstationary optimal servo control realizing smooth switching from velocity servo to position servo – experimental study," *IEEJ Trans. Electric. Electron. Eng.*, vol. 1, no. 3, pp. 349-352, 2006.

[7] S. Hara and Y. Yamada, "A control method switching from servo automatic transfer to force sensorless impedance control manual positioning," in *Proc. 33rd Annual Conf. IEEE Industrial Electronics Soc.*, Taipei, Taiwan, 2007, pp. 292-298.

[8] S. Hara, "Adaptive nonstationary positioning control of vibration systems by means of solutions of time-varying Riccati equations," *Microsyst. Technol.*, vol. 13, no. 8-10, pp. 1063-1075, 2007.

[9] S. Hara, "Adaptive nonstationary servo positioning control switching from velocity servo to position servo," in *Proc. 2007 American Control Conf.*, New York, NY, 2007, pp. 2232-2235.

[10] S. Hara, "Efficient design of time-varying gain type controller and positioning control of vibration systems - taking account of parameter variations -," *IEEJ Trans. Indust. Appli.*, vol. 125, no. 9, pp. 871-878, 2005.

[11] S. Tachi, T. Sakaki, H. Arai, S. Nishizawa, and J. F. Pelaez-polo, "Impedance control of a direct drive manipulator without using force sensors," *J. Robot. Soc. Jpn.*, vol. 7, no. 3, pp. 172-184, 1989.

[12] S. Hara, "A smooth switching from power-assist control to automatic transfer control and its application to a transfer machine," *IEEE Trans. Indust. Electron.*, vol. 54, no. 1, pp. 638-650, 2007.